Time Reversal of Elastic Waves in Soft Solids

S. Catheline,[1] N. Benech,[2] J. Brum,[2] and C. Negreira[2]

[1]*Laboratoire Ondes et Acoustique, ESPCI, Université Paris VII, U.R.A. C.N.R.S. 1503, 10 rue Vauquelin, 75231 Paris cedex 05, France*

[2]*Laboratorio de Acustica Ultrasonora, Instituto de fisica, Faculdad de ciencia, Universidad de la Republica, calle Igua Montevideo, Uruguay*

(Received 4 June 2007; revised manuscript received 13 December 2007; published 15 February 2008)

When a scalar far-field wave is time reversed, it starts to converge toward its initial point source location, then collapses and finally diverges. Without evanescent waves, the symmetric focus spot is limited by the Rayleigh criterion. We present an experimental observation of a time-reversal elastic wave in a soft solid cavity using the transient elastography technique. It is observed that the time-reversed far field wave collapses and gives birth to near fieldlike effects. Elastodynamic Green's functions computation confirms the experimental conclusions: the diffraction limit implies a direction dependant Rayleigh criterion.

DOI: 10.1103/PhysRevLett.100.064301 PACS numbers: 43.35.+d, 42.25.Fx, 43.20.+g, 43.80.+p

The potential of time-reversal (TR) methods includes different areas such as telecommunication [1,2], nondestructive testing [3], interactivity [4], medical imaging, and therapy [5]. It is an elegant and robust adaptive focusing method. In practical situations, a source or a strong reflector embedded in the medium is required in order to observe a forward wave scene. Then, a TR mirror is used to recreate the backward scene. The time-reversed wave finally collapses on its source location. The problem of the source in a TR experiment is known in the medical field [6] as the ''artificial ultrasonic stars'' in reference to analogous laser guided artificial stars used for optics adaptive focusing in astronomy [7]. In the TR experiments presented in this Letter, a reverberant solid cavity has been used. The great advantage of such configuration is that a perfect TR cavity can be approached experimentally using a point source and a point receiver: it is the so-called one channel time-reversal mirror [8]. The elastic field in volume was measured noninvasively from the solid surface using ultrasonic techniques developed in the field of transient elastography [9]. In this medical field, propagation media are soft solids such as soft tissues, muscles, organs [10], or mimicking tissue phantoms. The low frequency shear waves (a few hundred hertz) propagate at a speed of a few meters per second, which results in centimeter size wavelength. Consequently, the original aspects of these time-reversal elastography experiments are (1) no ''artificial stars'' are needed, (2) the time-reversal collapse is directly observed inside a solid, and (3) for centimeter wavelength, near fieldlike effects are clearly apparent. The experimental observations are compared with numerical computation of a perfect TR cavity based on elastodynamic Green's functions. Contrary to the case of fluids, the elastic field before and after the collapse differs, and the focus spot is no more isotropic. Its size remains, however, in the dimension of the wavelength in the absence of the high spatial frequencies of evanescent waves [11]. The nonisotropic shape of the focus spot merging from a homogeneous reverberating field might appear surprising at first sight. However, this observation follows the symmetry of the Green's functions and the nature of their simplest associated point sources in liquids and solids or more generally, in a scalar or an elastic field.

The linear system analysis point of view provides a straightforward mathematical description of time-reversal experiment in solid reverberant cavity. Let $\Psi_z(\vec{r}_0, t)$ be the z-component of the displacement field at a position $\vec{r}_0$ and time t. It is expressed as a time-convolution product between a source $e_k(\vec{r}_s, t)$ located in $\vec{r}_s$, oriented toward any direction k, and the impulse response between the k and z-components of the source and the receiver respectively $h_{kz}(\vec{r}_0, \vec{r}_s, t)$ (see Fig. 1 for axis definition):

$$\Psi_z(\vec{r}_0, t) = e_k(\vec{r}_s, t) \otimes_t h_{kz}(\vec{r}_0, \vec{r}_s, t). \quad (1)$$

In the experiment, Fig. 1, the source was a circular piston (5 mm radius) mounted on a vibrator (Bruel & Kjaer 4810

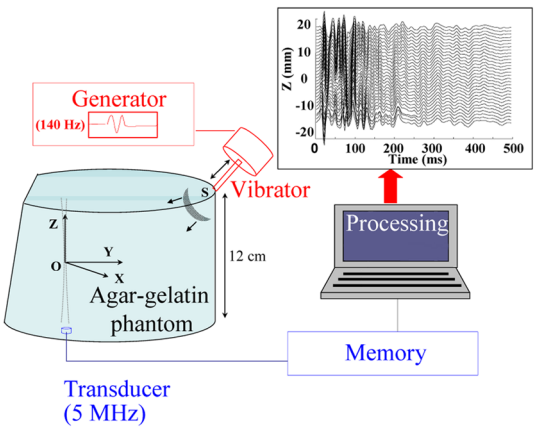

FIG. 1 (color online). Experimental Setup. An acoustic pulse sent by a piston vibrator generates motion in a soft solid. An ultrasonic device developed for transient elastography allows to measure the displacement field in volume, represented here as a seismogram.

type) and applied at the surface of a tissue mimicking agar-gelatin phantom (3% agar, 3% gelatin in water). The phantom had a cylinder shape of elevation 9 cm and diameter 12 cm. In order to attenuate geometrical effects due to high symmetry of the cylinder, a plan segment was cut off. Two cycles of sinusoid were sent in the audible range (150 Hz). The resulting vectorial field was measured in volume with an ultrasonic method [9]. It uses a 5 MHz ultrasonic transducer and a pulse-echo system storing 500 acoustic signals in memory at a 1000 Hz rate. Similarly to Doppler techniques, it delivers the component of the particle velocity of 30 tissue slices distributed on a 3.8 cm depth along the ultrasonic ray (z-axis). The resulting field is shown in a seismic-like representation, Fig. 1. Displacements are observed at time greater than the initial pulse duration ($\sim$7 ms). It indicates the presence of a reverberated field. Compared to other solid cavities [3,8], this field is dominated by shear waves [9]. The shear wave speed, $C_S \sim 3.35\ \mathrm{m\,s^{-1}}$, was measured with a classic time delay technique using transient elastography. With a central frequency $f_c \sim 105$ Hz, the shear wavelength estimation was 3.2 cm, much smaller than the compression wavelength ($\sim$15 m). The strong influence of viscous effects was estimated through the quality factor defined on the spectrum as the mean -6 dB width of resonances divided by their frequency ($Q \sim 10$). This low value was not prohibitive however for the realization of one-channel TR experiments. At last, it should be noted that compared to the mean shear wavelength, emission and reception can be regarded as pointlike.

Before presenting the TR experiments, a last consideration should be introduced. The space reciprocity of the elastic field applied to Eq. (1) yields to

$$\Psi_z(\vec{r}_0, t) = \Psi_k(\vec{r}_s, t) = e_z(\vec{r}_0, t) \otimes_t h_{zk}(\vec{r}_s, \vec{r}_0, t). \quad (2)$$

It results from now that $\vec{r}_s$ can be considered as a surface receiver position and $\vec{r}_0$ as a virtual source position embedded in the medium. From this point of view, the source position was arbitrarily chosen at the origin $z = 0$ mm. The corresponding surface displacement, of a total duration $T = 500$ ms, was time reversed, and reemitted from the surface by the vibrator: $e_k(\vec{r}_s, t) = \Psi_k(\vec{r}_s, T - t)$. The resulting time-reversed field inside the medium at position $\vec{r}$ is thus deduced from (1) and (2) as

$$\Psi_z^{\mathrm{TR}}(\vec{r}, t) = e_z(\vec{r}_0, T - t) \otimes_t h_{zk}(\vec{r}_s, \vec{r}_0, T - t) \otimes_t h_{kz}(\vec{r}, \vec{r}_s, t). \quad (3)$$

The novelty here is not in the use of the reciprocity, widely described in the TR literature. It resides in the volumic field measurement that nullifies the need for any "artificial star." This TR field was measured as a function of time along the z-axis of the transducer, $\vec{r} = z\vec{u}_z$. The spatio-temporal displacements are represented on a gray-color scale, Fig. 2. In agreement with theory, the spatio-temporal collapse occurs at time $t = T$ and on the source position $z = 0$. Thus, TR shear wave beam forming in soft tissues is envisioned as a first potential application [12]. The peak to background noise ratio can be estimated from the time field on the source position, -21 dB. This rather weak value accounts for the low quality factor of the cavity. On the other hand, the -6 dB width of the spatial refocusing at $t = 500$ ms is 3.4 cm, twice as big as the diffraction lower limit theoretically equal to half a wavelength, $\sim$1.6 cm. This observation is the first clue indicating that the Rayleigh criterion transposed to solids needs interpretation adjustments.

The TR collapse in the neighborhood of the source and around the time refocusing is now investigated. In order to discriminate the TR field from the random fluctuations of the reverberation, the experimental results had to be averaged. An easy way consists in replacing the real TR experiment by a TR field resulting from correlation computations of displacement measurements. Indeed, from (1), the expression of the correlation between the field measured on $\vec{r}$ and $\vec{r}_0$ is

$$C(\vec{r}_0, \vec{r}, t) = \Psi_z(\vec{r}_0, T - t) \otimes_t \Psi_z(\vec{r}, t). \quad (4)$$

As in (2), applying the reciprocity property to the first term of the convolution product gives

$$C(\vec{r}_0, \vec{r}, t) = \Psi_k(\vec{r}_s, T - t) \otimes_t \Psi_z(\vec{r}, t) = e_k(\vec{r}_s, t) \otimes_t \Psi_z^{\mathrm{RT}}(\vec{r}, t). \quad (5)$$

Consequently, for delta function emission, correlation and TR field are equal. However, the correlation approach offers the great advantage to replace in the averaging process the manual scanning by simple code loops on source positions $\vec{r}_0$. Thus, a pulse was applied from the surface, and the displacement field of 30 tissue slices along the ultrasonic beam was measured. Then, the transducer was moved on the x-axis by 2.5 mm step for another measurement, and so on. A scan of the field $\Psi_z(\vec{r}, t)$ generated by the vibrator located at a minimum distance

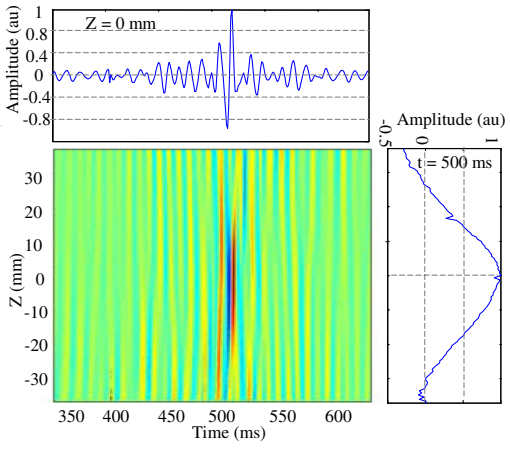

FIG. 2 (color online). Experimental Result. The time-reversal collapse on the initial source location is represented on a gray scale map. The spatial and temporal refocusing are shown at time $t = 500$ ms and depth $z = 0$ mm, respectively.

of 8 cm was finally stored in a $30 \times 30 \times 500$ matrix. This minimum distance between the emitting and the receiving point represents several shear wavelengths. Thus, measurements were done in the far field. Then, the correlation functions (4) were computed and summed over the possible source positions $\vec{r}_0$. Four pictures around the collapse time chosen as the origin were selected, Fig. 3. Although random fluctuations of the reverberation field are still present, the spatio-temporal collapse is clearly apparent at time $t = 0$ ms. A converging wave at time $t = -6$ ms and a diverging wave at time $+6$ ms and $+9$ ms are also visible. But they do not present the symmetric features of TR scalar fields issued from a simple source: the time-reversed wave energy is not homogeneously distributed on circles. As a result, a nonaxisymetric refocusing spot is found at time 0 ms. The -6 dB width along the z-axis (source direction) is 1.6 times bigger than in the x direction. They were found to be 2.1 and 1.3 cm, respectively. This latter value is very close to the shear half wavelength estimation, 1.2 cm ($F_c \sim 130$ Hz, $C_s = 3.35\ \mathrm{m\,s^{-1}}$). Consequently, a second potential application of this approach concerns the shear elasticity assessment through the wavelength estimation.

The pictures of Fig. 3 allow a convincing visual manifestation of near field waves. Indeed, it is important to keep in mind that the z-component of the displacement was measured. Therefore, along the z-axis, one observes a longitudinally polarized wave that propagates at the shear wave speed: it is a near field wave (e.g., [9,13]).

One may point out that the spatial asymmetry of the observed TR collapse results from the emission of an isotropic reverberating field. Thus, to go further in the comprehension of the symmetry properties of the focus spot, a perfect TR cavity was constructed using the Betti's theorem approach. In a first step, a body force $f_z(\vec{0}, 0)$ is set at the origin. Using the Green's function of elastodynamic [13], the i-component of the displacement field $u_i(\vec{r}_0, t)$ measured at the surface S of a TR cavity is

$$u_i(\vec{r}_0, t) = \iiint_V f_z(\vec{0}, 0) \otimes G_{zi}(\vec{r}_0, t; \vec{0}, 0) dV. \qquad (6)$$

The body force is supposed to be pointlike and to emit a delta function, $f_z(\vec{0}, 0) = \delta(\vec{r})\delta(t)$ so that (6) simplifies to $u_i(\vec{r}_0, t) = G_{zi}(\vec{r}_0, t; \vec{0}, 0)$. Some hypothesis about the TR cavity are introduced now: first the cavity has free boundary, and its surface is covered with ideal particle velocity sensors. Thus, once time reversed, the traction $T_i(\vec{r}_0, t)$ emitted from the TR cavity surface is $T_i^{\mathrm{TR}}(\vec{r}_0, t) = Z \frac{\partial u_i(\vec{r}_0, T-t)}{\partial t} = \frac{\partial G_{zi}(\vec{r}_0, T-t; \vec{0}, 0)}{\partial t}$, where the mechanical impedance Z is set to unity. In the absence of body- force, the field $u_z(\vec{r}, t) = \iint_S T_i(\vec{r}_0, t) \otimes G_{iz}(\vec{r}, t; \vec{r}_0, t_0) dS$ finally gives

$$u_z^{\mathrm{TR}}(\vec{r}, t) = \iint_S \frac{\partial G_{zi}(\vec{r}_0, T - t; \vec{0}, 0)}{\partial t} \otimes G_{iz}(\vec{r}, t; \vec{r}_0, t_0) dS. \qquad (7)$$

A similar approach is used in fluid with the Green's theorem [14]. Given the complexity of the Green's function in solids [13], Eq. (7) was computed numerically as follows. The TR cavity was a cube, 8 cm side. Control points for emission or reception were distributed along a mesh grid at interval of 0.2 cm. The physical parameters were all chosen equal to their estimation in the experiment: $\rho = 1000\ \mathrm{kg\,m^{-3}}$, $C_s = 3.35\ \mathrm{m\,s^{-1}}$, $C_p = 1500\ \mathrm{m\,s^{-1}}$, $f_c = 130$ Hz. A TR elastic *free* field in a *lossless* medium is thus computed. In a first step, a one cycle sinusoid $e(t)$ was sent from a point body force located in the center of the cavity, $x = y = z = 4$ cm, and oriented along the z-axis.

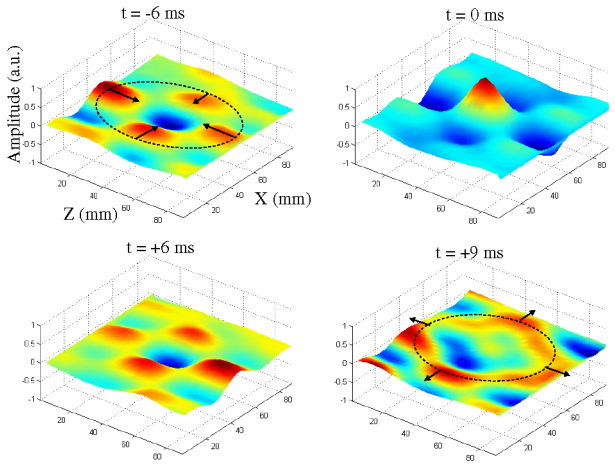

FIG. 3 (color online). Experimental Results. Four pictures of a time-reversal field computed from correlations were selected around the refocusing time, $t = 0$ ms. The initial point body force was aligned in the z direction. The z component of the displacement field is represented here. Arrows indicate the propagation direction.

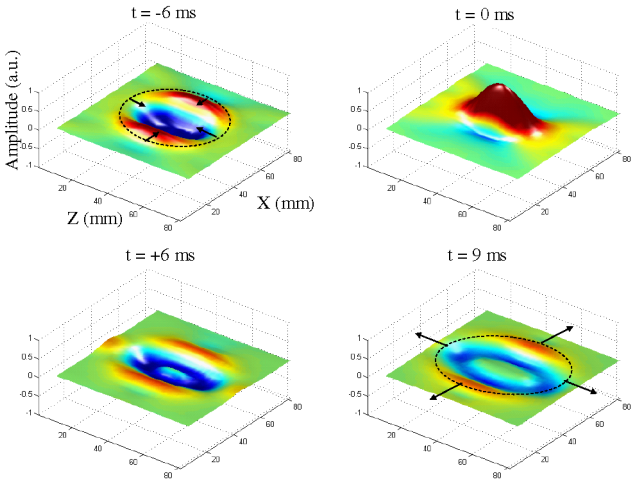

FIG. 4 (color online). Computation result using elastodynamic Green's function. Four pictures of the z-displacement field created by a perfect time-reversal cavity were selected around the refocusing time, $t = 0$ ms. The initial point body force was aligned in the z direction. Arrows indicate the propagation direction.

All the components of the field were computed from (6) on the 6 walls of the cubic cavity. This field was time differentiated and time reversed before being reemitted. The z-component of the time-reversed field was computed from (7). Four pictures around the collapse time were selected from the simulation movie, Fig. 4. The converging wave, the collapse, and the diverging wave are visible at time $t < 0$ ms, $t = 0$ ms, and $t > 0$ ms, respectively. A nonhomogeneous circular distribution of energy is observed, in agreement with experiments. The refocusing spot does not present a circular symmetry: the -6 dB width estimation gives 1.2 cm along the x-axis versus 2.5 cm along the z-axis. The ratio ~ 2 is slightly higher than in the experiment (1.6). The near field wave is clearly apparent as a longitudinally polarized shear wave along the z-axis. It decreases at a distance r from the source according to a typical $1/r^2$ law. Consequently, the computation results are fully compatible with the experimental analysis: by time reversing far field waves, it has been possible to recreate near fieldlike effects around a nonsymmetric focus spot. However, contrary to near field evanescent waves created by an acoustic sink, they do not involve subwavelength resolution.

The direction dependant resolution is a consequence of the point body-force radiation pattern. In the simple case of a monochromatic point body force, the free field radiation pattern can be computed analytically [15] and is demonstrated to have a cigar shape. Once time reversed, the symmetry features of the initial field are conserved, including in the experimental situation of an isotropic reverberation field. However, the smallest dimension of the refocusing spot remains of the order of half a wavelength, in good agreement with the Rayleigh criterion.

The absence of reverberation fluctuations in this ideal case brings one further feature: the time-reversed fields at -6 ms and $+6$ ms differ. Contrary to the case of a simple point source immersed in a fluid, it is not symmetric as respect to the refocusing time $t = 0$ ms. The simple point source designates the source for which the field is the Green's function [16]. This difference is thought to be closely related to the spatial symmetry of the source and more precisely to the nonisotropic radiation pattern of a point body force. This interpretation is based on the analysis of TR fields obtained with complex sources (composed of simple sources). For example, it can be proven that a dipole source in fluid generates a nonsymmetric TR field [15]. Inversely, a monopolar pulsing sphere in solid results in a symmetric TR field. Consequently, the lack of time symmetry with respect to the refocusing time reflects the spatial asymmetry of the emitted energy by the initial point body force, Fig. 4. It should be noted that this relationship between time and spatial symmetry is used in seismology: the causal symmetry of a TR coda wave field characterizes the spatial distribution of sources [17]. This open question should rigorously be analyzed in the frame of causal symmetry of propagators [18].

The TR analysis thus reveals the space symmetry properties of the source that are in turn linked in the present experiments to the fundamental nature difference of a simple point source in solids and in fluids. From a general point of view, extracting information from complex reverberant fields in the human body [19] is thought to be potentially useful for medicine as it is for seismology [20].

[1] G. Lerosey, J. de Rosny, A. Tourin, and M. Fink, Science **315**, 1120 (2007).

[2] W. A. Kuperman, W. S. Hodgkiss, H. C. Song, T. Akal, C. Ferla, and D. R. Jackson, J. Acoust. Soc. Am. **103**, 25 (1998).

[3] T. J. Ulrich, Paul A. Johnson, and Robert A. Guyer, Phys. Rev. Lett. **98**, 104301 (2007).

[4] R. K. Ing, N. Quieffin, S. Catheline, and M. Fink, Appl. Phys. Lett. **87**, 204104 (2005).

[5] J. L. Thomas, F. Wu, and M. Fink, Ultrason. Imag. **18**, 106 (1996).

[6] M. Pernot, G. Montaldo, M. Tanter, and M. Fink, Appl. Phys. Lett. **88**, 034102 (2006).

[7] L. A. Thompson and C. S. Gardner, Nature (London) **328**, 229 (1987).

[8] C. Draeger and M. Fink, Phys. Rev. Lett. **79**, 407 (1997).

[9] S. Catheline, F. Wu, and M. Fink, J. Acoust. Soc. Am. **105**, 2941 (1999).

[10] R. Muthupillari, D. J. Lomas, P. J. Rossman, J. F. Greenleaf, A. Manduca, and R. L. Ehman, Science **269**, 1854 (1995).

[11] J. de Rosny and M. Fink, Phys. Rev. Lett. **89**, 124301 (2002).

[12] Z. Wu, L. S. Taylor, D. J. Rubens, and K. J. Parker, J. Acoust. Soc. Am. **111**, 439 (2002).

[13] The elastodynamic Green's functions [e.g., K. Aki and P. G. Richards, *Quantitative Seismology* (Freeman, San Francisco, 1980), Vol. I, p. 73] are: $G_{ij} = (\vec{r}, t; \vec{0}, 0) = \frac{1}{4\pi\rho C_P^2}\frac{\gamma_i\gamma_j}{r}\delta(t - \frac{r}{C_P}) - \frac{1}{4\pi\rho C_S^2}\frac{(\gamma_i\gamma_j - \delta_{ij})}{r}\delta(t - \frac{r}{C_S}) + \frac{1}{4\pi\rho} \times \frac{(3\gamma_i\gamma_j - \delta_{ij})}{r^3}\pi_{t_S}^{t_P}$ where ρ and δ_{ij} stand for the density and the Kronecker symbol, respectively. $\gamma_j = \frac{x_i}{r}$ is the direction cosines, and $\pi_{t_S}^{t_P}$ is a gate function from arrival time $t_S = \frac{r}{C_S}$ to $t_P = \frac{r}{C_P}$.

[14] D. Cassereau and M. Fink, IEEE Trans. Ultrason. Ferroelectr. Freq. Control **39**, 579 (1992).

[15] See EPAPS document No. E-PRLTAO-100-068807 for video sequences of the TR experiment and simulation and for detailed computation of a monochromatic point body-force pattern in solids and of a TR field in fluids. For more information on EPAPS, see http://www.aip.org/pubservs/epaps.html.

[16] P. M. Morse, *Theoretical Acoustic* (Princeton, New Jersey, 1986), p. 309.

[17] A. Paul, M. Campillo, L. Margerin, E. Larose, and A. Derode, J. Geophys. Res. **110**, B08302 (2005).

[18] G. Barton, *Element of Green's Functionsand Propagation* (Oxford Science Publications, New York, 1989), p. 239.

[19] K. G. Sabra, S. Conti, P. Roux, and W. A. Kuperman, Appl. Phys. Lett. **90**, 194101 (2007).

[20] N. M. Shapiro, M. Campillo, L. Stehly, and M. H. Ritzwoller, Science **307**, 1615 (2005).